

## SEMANTIC INFORMATION EXTRACTION OF LANES BASED ON ONBOARD CAMERA VIDEOS

Luliang Tang<sup>1</sup>, Tuo Deng<sup>1,\*</sup>, Chang Ren<sup>1</sup>

<sup>1</sup> State Key Laboratory of Information Engineering in Surveying, Mapping, and Remote Sensing, Wuhan University, Wuhan, China - (tl, dengtuo, imrc)@whu.edu.cn

Commission III, WG III/1

**KEY WORDS:** Lane Marking Detection, Lane Semantic Recognition, Lane Classification, Onboard Camera Video, Lane-Based Road Network

### ABSTRACT:

In the field of autonomous driving, semantic information of lanes is very important. This paper proposes a method of automatic detection of lanes and extraction of semantic information from onboard camera videos. The proposed method firstly detects the edges of lanes by the grayscale gradient direction, and improves the Probabilistic Hough transform to fit them; then, it uses the vanishing point principle to calculate the lane geometrical position, and uses lane characteristics to extract lane semantic information by the classification of decision trees. In the experiment, 216 road video images captured by a camera mounted onboard a moving vehicle were used to detect lanes and extract lane semantic information. The results show that the proposed method can accurately identify lane semantics from video images.

### 1. INTRODUCTION

High-precision lane-level road maps provides information such as lane number, location, geometry and connectivity semantic, and its acquisition of low cost is a focus and difficulty in the field of autonomous driving (Hillel et al, 2014). There are several existing methods for obtaining lane-level road information: such as using high resolution images to extract the centerline markings and the width of lanes (Ye et al, 2006; Cao et al, 2017; Yu et al, 2013; Lisini 2006); using airborne/terrestrial Lidar data to extract the edge, road markings and geographic position of lanes(Fang et al, 2013; Anttoni et al, 2008; Hui et al, 2016); using GPS trajectories to extract the number, location, and change detection of lanes(Chen et al, 2010; Tang et al, 2016; Yang et al, 2017). The above lane-level road data acquisition methods have the disadvantages of high cost, slow update, lack of semantic information, so it is urgent to develop a method with low cost, quick collection, and complete road information.

With the rapid development of sensors and Internet of Things technologies, more and more vehicle users have installed onboard cameras. These videos produced huge amounts of video data, containing rich road markings and lane semantic information such as speed limit signs, lane direction, and turning information (Yeh et al, 2015). Therefore, onboard camera videos data provides a rich data source for lane-level road information extraction with fast acquisition, low cost, and complete semantic information, which provides important technical support for vehicle navigation, driving assistance system, and autonomous driving. The onboard camera videos are mainly used for lane detection in driving assistance system in the existing research (Aly, 2008; Paula et al, 2013; Chen et al, 2011). There is less research on lane semantic recognition. This

paper proposes a method of extracting lane position and semantic information by using onboard camera videos.

### 2. TYPE OF LANE MARKINGS

There are many types of lanes on the road surface, and different lane markings represent different traffic regulations. According to the urban road planning and construction standards, the types of lane markings are divided into the following twelve types (Figure 1): solid white lines, dashed white lines, double solid white lines, solid-dashed white lines, dashed-solid white lines, double dashed white lines, solid yellow lines, dashed yellow lines, double solid yellow lines, solid-dashed yellow lines, dashed-solid yellow lines, double dashed yellow lines.

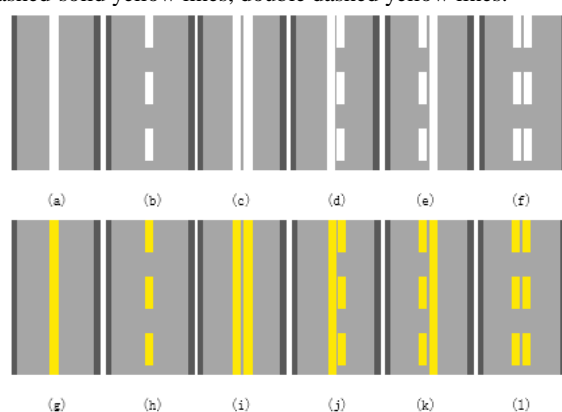


Figure 1. Types of lane markings: (a)solid white(b)dashed white(c)double solid white(d)solid-dashed white(e)dashed-solid white(f)double dashed white(g)solid yellow(h)dashed yellow(i)double solid yellow(j)solid-dashed yellow(k)dashed-solid yellow(l)double dashed yellow

\* Corresponding author

In general, white lines always separates traffic in the same direction while yellow lines separates the inverse. Single dashed lines mean passing or lane changing is allowed, single solid white lines mean lane changing is discouraged but not prohibited, and double solid white lines mean it is prohibited. On two-lane roads, a single dashed centerline means that passing is allowed in either direction, a double solid centerline means passing is prohibited in both directions, and the combination of a solid line with a dashed line means that passing is allowed only from the side with the broken line and prohibited from the side with the solid line.

### 3. SEMANTIC INFORMATION EXTRACTION OF LANES

#### 3.1 Lane Markings Detection Based on Videos

Detecting lane markings is the basis of extracting lane semantic information, so the first step of the proposed approach is to detect lane boundaries from video images. To simplify complicated lane detection problem, we assume the following conditions: (1) strong image noise does not exist; (2) the road width is fixed or changes slowly and the road plane is flat; (3) the camera frame axis stays parallel to the road frame plane. These assumptions can improve the effectiveness and real-time performance of the detection algorithm.

The flow diagram of the whole detection algorithm is shown in Figure 2. First, the input road images need be preprocessed, including selecting the road portion of images as the Region of Interest (ROI), converting RGB images into YUV colour space and median filtering. Second, the gradient direction feature is applied to the processed images to detect lane boundaries. Subsequently, binary images of lane boundary points are acquired.

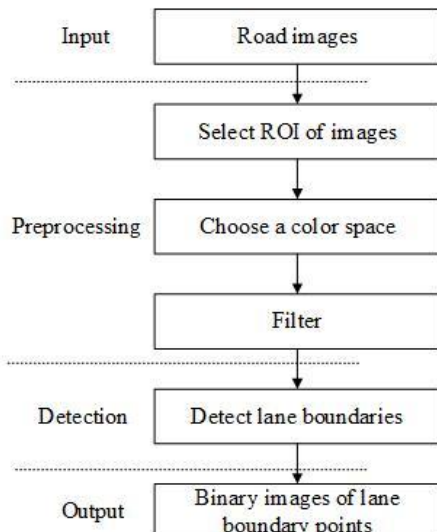


Figure 2. Flow diagram of the whole detection algorithm

Lanes in the road images have the feature of extending in the vertical direction, so we use the grayscale feature in the horizontal direction to detect lane edges. Figure 3 is the grayscale of pixel points in the horizontal direction selected from the image. There are four points have a sudden increase in the grayscale compared to the previous point, which correspond to the left edge of the lane markings in the road image. There are four points have a sudden decrease in the grayscale

compared to the previous point, which correspond to the right edge.

We assume that the grayscale of the pixel point  $(x, y)$  in the image is  $L(x, y)$ , and define the gray differential value in the horizontal direction  $\Delta L(x, y)$  is:

$$\Delta L(x, y) = L(x, y) - L(x+1, y) \quad (1)$$

Figure 4 is the grayscale differential values in the horizontal direction. In this paper, only the right edge of the lane is considered, so the negative values are ignored. The edge points of the lane are not only satisfied that the grayscale is significantly larger than the grayscale of non-lane points, but also have the characteristic that the grayscale significantly decrease at the edge of the lane. Therefore, the edge points of the lane can be detected by using the characteristic of the grayscale differential value. The grayscale threshold and the grayscale differential value threshold are respectively represented by  $T$  and  $\Delta T$ . When  $L(x, y) > T$  and  $\Delta L(x, y) > \Delta T$  are both satisfied, the pixel point is considered as an edge point of lane markings.

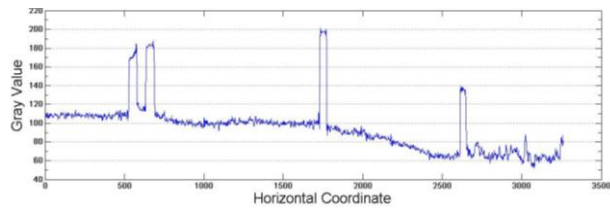


Figure 3. The grayscale corresponding to the pixels on the horizontal axis

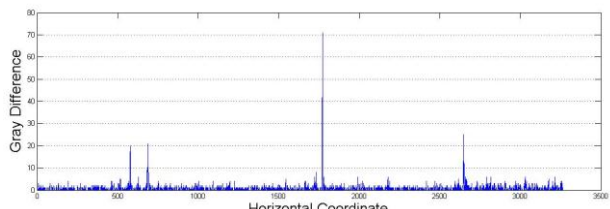


Figure 4. Grayscale differential value in the horizontal direction

#### 3.2 Lane Recognition

##### 3.2.1 Lane Boundary Fitting:

After getting the binary image of the edge points, these edge points are needed to be fitted into lines. There are many researches and models on lane markings fitting. The simpler models include mathematical models such as linear, quadratic and cubic fitting. The more complex models include B-Snake and Catmull-Rom Spline (Geng et al, 2011).

In this paper, the improved Probabilistic Hough transform is used to fit the lane markings. The results of the original Hough transform method are greatly affected by the threshold and the fitting results often contain mistakes such as containing some non-lane markings or fitting repeatedly. We add the slope feature of the lines into Hough transform, combine the straight lines whose slope differential value is less than the threshold range, and finally obtain the more correct lane lines. Figure 5 shows the result of lane line fitting in one road image.



Figure 5. An example of lane boundary fitting

### 3.2.2 Imaging Model of the Onboard Camera

The imaging model of the camera describes the mapping relationship between the 2-D coordinates of the points on the captured road images and the 3-D coordinates of those points. Five coordinate systems are included in this experiment:

(1)Pixel Coordinate System: The upper left corner of the image is the origin of the coordinate, and the  $u$  axis and the  $v$  axis respectively correspond to the columns and rows in the image array.

(2)Image Coordinate System: This coordinate uses the principal point as the origin. The  $X$  axis is parallel to  $u$  axis of the pixel coordinate and the  $Y$  axis is parallel to  $v$  axis.

(3)Camera Coordinate System: This coordinate uses the Projection Center of the camera as the origin.  $X_c$  axis and  $Y_c$  axis are respectively parallel to  $X$  axis and  $Y$  axis of the image coordinate, and  $Z_c$  axis is the optical axis of the camera.

(4)Car Coordinate System: The intersection of the car's vertical centerline and the road surface is the origin.  $X_v$  axis points to the front of the vehicle's vertical axis, which is parallel to the car's driving direction.  $Y_v$  axis points to the right of the vehicle's vertical axis.  $Z_v$  axis points above the vehicle's vertical axis.

(5)World Coordinate System: This coordinate defines the locations of object points in the 3-D space. Beijing 1954 Gauss Kruger projection coordinate system and WGS-1984 geographic coordinate system are adopted. The points of lanes are finally represented by the WGS-1984 geographic coordinate.

The imaging process of the camera is the conversion between each coordinate system. It is important to figure out coordinate transformation before camera calibration. Pixel coordinate is converted to image coordinate:

$$\begin{cases} x = (u - u_0)d_x \\ y = (v - v_0)d_y \end{cases} \quad (2)$$

where  $x, y$  = image coordinates

$u, v$  = pixel coordinates

$u_0, v_0$  = principal point coordinates

$d_x, d_y$  = the physical dimensions of  $X$  axis and  $Y$  axis

Transformation between image coordinate and camera coordinate is:

$$\begin{cases} x = f_i d_x y_c / x_c \\ y = -f_j d_y z_c / x_c \end{cases} \quad (3)$$

where  $f_i, f_j$  = focal length

$x_c, y_c, z_c$  = camera coordinates

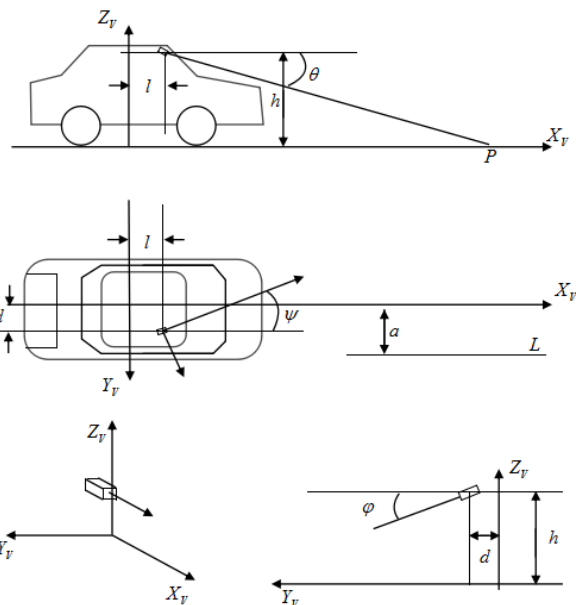


Figure 6. The relationship between camera coordinate and car coordinate

The direction angle  $\psi$  is a rotation angle between the main optical axis of the camera and the  $X_v$  axis of the car coordinate, whose positive direction points to the left side of the car. The roll angle  $\varphi$  is a rotation angle between the main optical axis and the  $Y_v$  axis, whose positive direction is clockwise. The pitch angle  $\theta$  is around the  $Z_v$  axis, whose positive direction is above the vertical axis of the car. The position of the optical centre in car coordinate system is  $t = (l, h, d)$ . The transformation between car coordinate system and camera coordinate system can be represented by  $R$  and  $t$ :

$$P_v^T = R \cdot P_c^T + t^T \Leftrightarrow P_c^T = R^{-1} \cdot P_v^T - R^{-1} \cdot t^T = R^T \cdot P_v^T - R^T \cdot t^T \quad (4)$$

where  $P_v$  = car coordinates

$P_c$  = camera coordinates

$$R = \begin{bmatrix} \cos \theta \cos \varphi & \sin \varphi \cos \psi + \cos \varphi \sin \psi \sin \theta & \sin \varphi \sin \psi - \cos \varphi \cos \psi \sin \theta \\ -\sin \theta \cos \varphi & \cos \varphi \cos \psi - \sin \varphi \sin \psi \sin \theta & \cos \varphi \sin \psi + \sin \varphi \cos \psi \sin \theta \\ \sin \theta & -\cos \theta \sin \psi & \cos \theta \cos \psi \end{bmatrix}$$

$$= \begin{bmatrix} r_{11} & r_{12} & r_{13} \\ r_{21} & r_{22} & r_{23} \\ r_{31} & r_{32} & r_{33} \end{bmatrix}$$

There is a translation and rotation relationship between the world coordinate system and the car coordinate system. The angle between the  $X_v$  axis and the  $X_w$  axis of the world coordinate system is  $\alpha$ , and the conversion relationship is:

$$\begin{cases} x_w = x_v \cos \alpha - y_v \sin \alpha + X_w \\ y_w = x_v \sin \alpha - y_v \cos \alpha + Y_w \end{cases} \quad (5)$$

where  $x_w, y_w$  = world coordinates

$x_v, y_v$  = car coordinates

$(X_w, Y_w)$  can be obtained by the camera. A can be calculated by two adjacent images:

$$\alpha = \arctan \left( \frac{Y_{w2} - Y_{w1}}{X_{w2} - X_{w1}} \right) \quad (6)$$

where  $X_{w1}, Y_{w1}$  = the current image coordinates  
 $X_{w2}, Y_{w2}$  = the next image coordinates

### 3.2.3 Calculate the Position of Lanes

There are six parameters describing imaging posture and location of the camera: 3 rotation angle- direction angle  $\psi$ , roll angle  $\varphi$  and pitch angle  $\theta$ , and 3 translation components-  $l$ ,  $d$  and  $h$ . This paper uses the vanishing point principle to calibrate camera parameters and does not require a specific calibration field. In accordance with the perspective projection principle of camera, three mutually non-coincident parallel lines have same vanishing point and different slopes on imaging plane (Li et al, 2004). Thus, the external parameters of the camera can be represented by a mathematical expression associated with parallel lane markings and vanishing point.

For a random line L parallel to the  $X_v$  axis, if the distance from L to  $X_v$  is  $a$ , the equation in the car coordinate system can be expressed as:

$$x_v = s, y_v = a, z_v = 0 \quad (7)$$

where  $a$  = any real number

To image this line, it needs to be transformed into the camera coordinate system. From (4), the equation of L in the camera coordinate system is:

$$\begin{bmatrix} x_c \\ y_c \\ z_c \end{bmatrix} = \begin{bmatrix} r_{11} & r_{21} & r_{31} \\ r_{12} & r_{22} & r_{32} \\ r_{13} & r_{23} & r_{33} \end{bmatrix} \begin{bmatrix} s \\ a \\ 0 \end{bmatrix} - \begin{bmatrix} r_{11} & r_{21} & r_{31} \\ r_{12} & r_{22} & r_{32} \\ r_{13} & r_{23} & r_{33} \end{bmatrix} \begin{bmatrix} l \\ d \\ h \end{bmatrix} \quad (8)$$

Finally, it is transformed into image coordinate system. From (3) and (8), the equation of L in the image coordinate system is:

$$\begin{cases} x = f_i d_x (sr_{12} + ar_{22} - lr_{12} - dr_{22} - hr_{32}) / (sr_{11} + ar_{21} - lr_{11} - dr_{21} - hr_{31}) \\ y = -f_j d_y (sr_{13} + ar_{23} - lr_{13} - dr_{23} - hr_{33}) / (sr_{11} + ar_{21} - lr_{11} - dr_{21} - hr_{31}) \end{cases} \quad (9)$$

The vanishing point of L in the image coordinate system is  $(u_h, v_h)$ . Because  $s$  is an any real number and the distance between the optical center of the camera in  $X_v$  axis is  $l$ , there is an any real number after adding or subtracting between  $s$  and  $l$ :

$$\begin{cases} u_h = \lim_{s \rightarrow \infty} u = f_i d_x (\sin \varphi \cos \psi + \cos \varphi \sin \psi \sin \theta) / \cos \theta \cos \varphi \\ v_h = \lim_{s \rightarrow \infty} v = -f_j d_y (\sin \varphi \sin \psi - \cos \varphi \cos \psi \sin \theta) / \cos \theta \cos \varphi \end{cases} \quad (10)$$

If there are at least three lane markings parallel to  $X_v$  on the road surface, the distance between them and  $X_v$  axis is  $a_1$ ,  $a_2$  and  $a_3$ . Their vanishing point is:

$$u_{h1} = u_{h2} = u_{h3} = u_h, \quad v_{h1} = v_{h2} = v_{h3} = v_h \quad (11)$$

The slope of the three lines can be computed:

$$g_n = -\frac{f_i d_x}{f_j d_y} \frac{a_n r_{12} r_{21} - dr_{12} r_{21} - hr_{12} r_{31} - ar_{11} r_{22} + dr_{11} r_{22} + hr_{11} r_{32}}{a_n r_{13} r_{21} - dr_{13} r_{21} - hr_{13} r_{31} - ar_{11} r_{23} + dr_{11} r_{23} + hr_{11} r_{33}} \quad n=1, 2, 3 \dots \quad (12)$$

Rotation angles  $\psi$ ,  $\varphi$  and  $\theta$ , and translation components  $l$ ,  $d$  and  $h$  can be computed:

$$\left\{ \begin{array}{l} \psi = \arctg \left( \left( (r_1 - r_3)(a_1 - a_2) - (r_1 - r_2)(a_1 - a_3) \right) / \left( (r_1 - r_3)(r_1 a_1 - r_3 a_2) - (r_1 - r_2)(r_1 a_1 - r_3 a_3) \right) \right) \\ \theta = \arctg \left( u_h \sin \psi / f_i d_x + v_h \cos \psi / f_j d_y \right) \\ \varphi = \arctg \left( \cos \theta \left( u_h / f_i d_x - \sin \psi \operatorname{tg}(\theta) \right) / \cos \psi \right) \\ h = (a_2 - a_1) AC / (BC - AD) \\ d = (B/A)(a_2 - a_1) AC / (BC - AD) + a_1 \end{array} \right. \quad (13)$$

where  $A = r_1 \sin \psi \cos \theta - \cos \theta \cos \psi$

$$B = -(\cos \varphi \sin \psi + \sin \varphi \cos \psi \sin \theta) - r_1 (\cos \varphi \cos \psi - \sin \varphi \sin \psi \sin \theta)$$

$$C = r_2 \sin \psi \cos \theta - \cos \theta \cos \psi$$

$$D = -(\cos \varphi \sin \psi + \sin \varphi \cos \psi \sin \theta) - r_2 (\cos \varphi \cos \psi - \sin \varphi \sin \psi \sin \theta)$$

$$r_n = -\left( f_j / f_i \right) (i_h - i_n) / (j_h - j_n), n=1, 2, 3 \dots$$

From(13), when we know the camera internal parameters  $f_i, f_j$  and  $u_0, v_0$ , the distance between any three lane markings on video images in the car coordinate system and  $X_v$  axis-  $a_1, a_2$  and  $a_3$ , and any other points on the three lanes in pixel coordinate system, the external parameters of camera can be calculated.

When calibration parameters of the camera are calculated, we can calculate the position of lane points by the coordinate transformation. On the assumption of flat road plane ( $z_v=0$ ), we can get from (4) and (9):

$$\begin{aligned} x_c &= -h / \left( r_{31} + (r_{32} u) / f_i d_x + (r_{33} v) / -f_j d_y \right) \\ y_c &= (x_c u) / (f_i d_x) \\ z_c &= (x_c v) / (f_j d_y) \end{aligned} \quad (14)$$

The coordinates of the lane points in the car coordinate system:

$$\begin{cases} x_v = r_{11} \left( -h / \left( r_{31} + (r_{32} u) / f_i d_x + r_{33} v / -f_j d_y \right) \right) + r_{12} \left( (x_c u) / (f_i d_x) \right) + r_{13} \left( (x_c v) / (f_j d_y) \right) + l \\ y_v = r_{21} \left( -h / \left( r_{31} + (r_{32} u) / f_i d_x + r_{33} v / -f_j d_y \right) \right) + r_{22} \left( (x_c u) / (f_i d_x) \right) + r_{23} \left( (x_c v) / (f_j d_y) \right) + d \end{cases} \quad (15)$$

### 3.3 Semantic Information Extraction of Lanes

#### 3.3.1 Lane Characteristics Analysis

The lane semantic information is obtained according to the types of lane markings. Lane markings have colour features, single or double line features, and dashed or solid line features. The traffic semantics represented by different types of lane markings are different. The two colours of the lines are white and yellow. It is found that the Cb component value of the yellow lane line under various lighting conditions is the smallest. So the Cb component  $I_{Cb}$  in the YCbCr colour space of the lane edge points can identify the colour. The white line is usually the dividing line between lanes running in the same direction, and the yellow line is the dividing line between lanes that drive in opposite directions. In order to distinguish single line or double line, it is necessary to use the actual distance value Id of the lane to judge. Define a ratio  $I_{ratio}$ , which means that the number of points on each lane line in the road binary image with the value of 255 is divided by the number of all

points on the straight line where the lane line is located.  $I_{ratio}$  is used to distinguish dashed line, solid line or double solid line, double dashed line, solid-dashed line/dashed-solid line. The solid-dashed line and the dashed-solid line are distinguished by the relative position. On the side of the solid line, the vehicle is not allowed to overtake, change the lane or turn around, while on the side of the dashed line the vehicle is allowed to overtake, change lanes or turn around in a safe condition. As shown in figure 7, carriageway (a) is composed of Lane1 and Lane2. Double solid yellow line on the left of Lane1, used to separates traffic in the inverse direction, while the dashed white line on the right of Lane1, used to separates traffic in the same direction. Therefore, Lane1 means that you can't turn left but you can turn right. On the right side of the Lane2 lane is the solid white line, which is the boundary line of the road. Lane2 means that you can't turn right but can turn left. The carriageway (b) is composed of Lane3 and Lane4. Left lane marking of Lane3 is same with Lane1, and the right lane marking of Lane3 is dashed white line, so it can turn right. The left lane marking of Lane4 is a solid-dashed white line, so it is not allowed to turn left because it is closer to the solid line. Lane3 means that you can't turn left but can turn right, and Lane4 means that you can't turn left but can turn right.

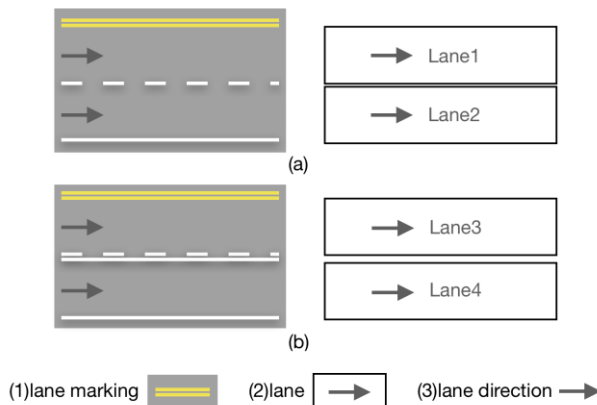


Figure 7. An example of semantic information extraction of lanes

### 3.3.2 Lane Semantic Information Extraction by Classification of Decision Trees

Decision tree model is a top-down tree structure in which each internal node represents an attribute of data, each branch represents a judgement, and each leaf node represents a class label. The top node of the tree is the root node of the decision tree (Friedl et al, 1999). We use a decision tree model to classify the lane markings into the following twelve types: solid white lines, dashed white lines, double solid white lines, solid-dashed white lines, dashed-solid white lines, double dashed white lines, solid yellow lines, dashed yellow lines, double solid yellow lines, solid-dashed yellow lines, dashed-solid yellow lines, double dashed yellow lines. First, determine the colour of the lane markings: as the value  $I_{ch}$  is larger than the threshold value  $T_1$ , the colour of lane markings is white, otherwise the colour is yellow. Then, as the value  $I_d$  is larger than the threshold value  $T_2$ , it is a single line, otherwise it is a double line. Using  $I_{ratio}$  to distinguish single dashed lines and single solid lines, distinguish double solid line, double dashed line, dashed-solid line/solid-dashed line. As the value  $I_{ratio}$  is larger

than the threshold value  $T_3$ , it is a solid line, otherwise it is a dashed line. As the value  $I_{ratio}$  is larger than the threshold value  $T_4$ , it is a double solid line; while the value  $I_{ratio}$  is less than the threshold value  $T_5$ , it is a double dashed line; the rest is dashed-solid lines and solid-dashed lines. Finally, we distinguish dashed-solid line and solid-dashed line by judging the left line of double line, the value  $I_{ratio}$  of the left line of double line is larger than the threshold value  $T_3$ , it is a solid-dashed line, otherwise it is a dashed-solid line. Decision tree model is shown in figure 8.

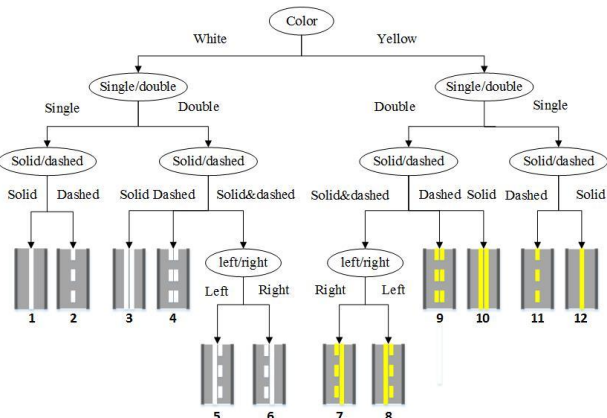


Figure 8. The decision trees model

## 4. EXPERIMENTAL ANALYSIS

The experimental data in this paper is a road video from a mobile phone. The phone is fixed in front of the car's windshield, and its video is the road ahead of the driving car. The time interval between the selected video images was 2 seconds. There are 216 images, and the resolution of each image is 3264\*2448. Each image has a location coordinate. The experimental area was Bayi Road in Wuhan. The road surface is flat, and the road condition is better because of few cars.

### 4.1 Lane Location Results

After calculating the six parameters describing imaging posture and location of the camera, input the detected lane marking edge points which are pixel coordinates, then get the final WGS-1984 geographic coordinates. In this paper, the centerlines of the left and right lane markings are used to represent the lanes. The real coordinates of the lane centerline are calculated. The results of one section of the road test are shown in Figure 9. Because there is no real accurate lane reference data, this paper converts the lane centerlines data into Keyhole Markup Language (KML) files for using Google Earth. We can have a qualitative accuracy evaluation with the images in Google Earth. Figure 9(b) is a partial enlarged view of the results. We can see that the positional deviation between the lane we calculated and the lane in the image is very small.



(a) An example of lane location results



(b) An example of superposition results of lane centerlines on Google Earth.

Figure 9. Lane location results

## 4.2 Lane Semantic Extraction Results

Sampling method is used to obtain the optimal threshold in the experiment, and statistics are made for the correct rate of decision tree classification under different thresholds. Among the 216 images, 186 of them can be correctly detected. Therefore, 120 of these correctly detected numbers are used as the training set of the decision tree classifier, and the remaining 66 are used as test sets. Tests have shown that when  $T_1=100$ ,  $T_2=1.5$ ,  $T_3=0.9$ ,  $T_4=1.8$ ,  $T_5=1.2$ , the best classification results are obtained. In the 66 road images, there are 3 classification objects for each, so there are a total of 198 test subjects. In the experiment, 182 objects were accurately identified and the recognition accuracy was 91.92%. Fig. 10 shows the lane recognition results of various semantics in the test section. As can be seen from Fig. 10, the method can recognize the lane semantics better. The figures identified in the images corresponds to the type of lane type in Fig. 8. The main reason for wrong identification is solid white, which is similar to double dashed white. This wrong identification needs to be improved.



Figure 10. Examples of accurate lane semantic extraction

## 4.3 Evaluation on the experiment method

The results of this paper are compared with a method to lane markings real-time detection (Aly, 2008) and a method of real-time detection and classification to lane markings detection (Paula et al, 2013). The comparison results of the three methods are shown in table 1. Aly's Method is based on generating a top view of the road, filtering using selective oriented Gaussian filters, using RANSAC line fitting. This algorithm can detect all lanes in images of the street in various conditions, but it can't locate the lane and extract the semantic information. Paula's method adopted a cascade of binary classifiers to distinguish markings, but it only have five types-dashed, dashed-solid, solid-dashed, single-solid and double-solid. This method can't extract the semantic information or locate lanes. This paper proposes a method of extracting lane position and semantic information, which benefits to the research on high-precision lane-level road maps.

Method	Detection accuracy	Lane location	Lane classification	Lane semantic extraction
Aly's	85%-90%	✗	✗	✗
Paula's	85%-90%	✗	88.30%	✗
Proposed	85%-90%	✓	91.92%	✓

Table 1. Comparison of experimental results

## 5. CONCLUSION

Based on the detection of lane markings in video images, this paper proposes a method of lane detection and semantic information extraction. The method starts from the detection and fitting of lane marking edges in the road images, calculates the lane position by vanishing point principle, and uses the decision tree classification method to identify the lane semantic information.

The method presented in this paper still has some drawbacks. It has poor detection results for the lane markings of roads or road intersections with large numbers of vehicles, affecting the subsequent results of lane positioning and semantic recognition. In the future, it will further improve the detection of lane markings in more complicated environment, detect road signs to increase the steering information of lanes, and complete lane-level road maps information.

## ACKNOWLEDGEMENTS

This work was supported by the grants from National Key Research and Development Plan of China (2017YFB0503604, 2016YFE0200400), the grants from the National Natural Science Foundation of China (41671442, 41571430, 41271442), and the Joint Foundation of Ministry of Education of China (6141A02022341).

## REFERENCES

- Hillel, A. B., Lerner, R., Dan, L., Raz, G., 2014. Recent progress in road and lane detection. *Machine Vision & Applications*, 25(3), pp. 727-745.
- Ye, M., Su, L., Li, S., Tang, J., 2006. Review and thought of road extraction from high resolution remote sensing images. *Remote Sensing For Land& Resources*, (1), pp. 12-17.
- Cao, Y., Wang, Z., Tang, L., 2017. Advances in method on road extraction from high resolution remote sensing images. *Remote Sensing Technology and Application*, 32(1), pp. 20-26.
- Yu, J., Yu, F., Zhang, J., Liu, Z., 2013. High resolution remote sensing image road extraction combining region crowding and road-unit. *Geomatics and Information Science of Wuhan University*, 38(7), pp. 761-764.
- Lisini, G., Tison, C., Tupin, F., Gamba, P., 2006. Feature fusion to improve road network extraction in high-resolution SAR images. *IEEE Geoscience & Remote Sensing Letters*, 3(2), pp. 217-221.
- Fang, Li., Yang, B., 2013. Automated extracting structural roads from mobile laser scanning point clouds. *Acta Geodaetica et Cartographica Sinica*, 42(2), pp. 260-267.
- Anttoni, J., Juha, H., Hannu, H., Antero, K., 2008. Retrieval algorithms for road surface modelling using laser-based mobile mapping. *Sensors*, 8(9), pp. 5238.
- Hui, Z., Hu, Y., Jin, S., Yao, Z. Y., 2016. Road centerline extraction from airborne lidar point cloud based on hierarchical fusion and optimization. *ISPRS Journal of Photogrammetry & Remote Sensing*, 118, pp. 22-36.
- Chen, Y., Krumm, J., 2010. Probabilistic modeling of traffic lanes from GPS traces. *Sigspatial International Conference on Advances in Geographic Information Systems ACM*, pp. 81-88.
- Tang, L., Yang, X., Dong, Z., Li, Q., 2016. CLRIC: collecting lane-based road information via crowdsourcing. *IEEE Transactions on Intelligent Transportation Systems*, 17(9), pp. 2552-2562.
- Yang, X., Tang, L., Stewart, K., Dong, Z., Zhang, X., Li, Q., 2017. Automatic change detection in lane-level road networks using GPS trajectories. *International Journal of Geographical Information Science*, (12), pp. 1-21.
- Yeh, A. G. O., Zhong, T., Yue, Y., 2015. Hierarchical polygonization for generating and updating lane-based road network information for navigation from road markings. *International Journal of Geographical Information Science*, 29(9), pp. 1509-1533.
- Aly, M., 2008. Real time detection of lane markers in urban streets. *IEEE Intelligent Vehicles Symposium*, pp. 7-12.
- Paula, M. B. D., Jung, C. R., 2013. Real-time detection and classification of road lane markings. *XXVI Conference on Graphics*, pp. 83-90.
- Chen, L., Li, Q., Mao, Q., 2011. Lane detection and following algorithm based on imaging model. *China Journal of Highway and Transport*, 24(6), pp. 96-102.
- Xun, G., Ming, Z., Zhao, F., 2010. *Digital photogrammetry*. The Mapping Publishing Company, pp. 28-40.
- Li, Q., Zheng, N., Zhang, X., 2004. Calibration of external parameters of vehicle-mounted camera with trilinear method. *Opto-Electronic Engineering*, 31(8), pp. 23-26.
- Friedl, M., Brodley, C. E., Strahler, A. H., 1999. Maximizing land cover classification accuracies produced by decision trees at continental to global scales. *IEEE Transactions on Geoscience & Remote Sensing*, 37(2), pp. 969-977.

*Revised March 2018*